Naval Research Laboratory

Washington, DC 20375-5320

NRL/MR/6400--11-9335

Spontaneous Transition of Turbulent Flames to Detonations in Unconfined Media

Alexei Y. Poludnenko

Laboratory for Computational Physics and Fluid Dynamics

Thomas A. Gardiner

Sandia National Laboratories
Albuquerque, New Mexico

Elaine S. Oran

Laboratory for Computational Physics and Fluid Dynamics

June 7, 2011

REPORT DOCUMENTATION PAGE

Form Approved
OMB No. 0704-0188

1. REPORT DATE *(DD-MM-YYYY)*	**2. REPORT TYPE**	**3. DATES COVERED** *(From - To)*
07-06-2011	Memorandum Report	

4. TITLE AND SUBTITLE

Spontaneous Transition of Turbulent Flames to Detonations in Unconfined Media

5a. CONTRACT NUMBER

5b. GRANT NUMBER

5c. PROGRAM ELEMENT NUMBER

6. AUTHOR(S)

Alexei Y. Poludnenko, Thomas A. Gardiner,* and Elaine S. Oran

5d. PROJECT NUMBER

5e. TASK NUMBER

5f. WORK UNIT NUMBER

64-4465-01

7. PERFORMING ORGANIZATION NAME(S) AND ADDRESS(ES)

Naval Research Laboratory, Code 6404
4555 Overlook Avenue, SW
Washington, DC 20375-5344

8. PERFORMING ORGANIZATION REPORT NUMBER

NRL/MR/6400--11-9335

9. SPONSORING / MONITORING AGENCY NAME(S) AND ADDRESS(ES)

10. SPONSOR / MONITOR'S ACRONYM(S)

11. SPONSOR / MONITOR'S REPORT NUMBER(S)

12. DISTRIBUTION / AVAILABILITY STATEMENT

Approved for public release; distribution is unlimited.

13. SUPPLEMENTARY NOTES

*Sandia National Laboratories, Albuquerque, NM 87185-1189

14. ABSTRACT

Deflagration-to-detonation transition (DDT) can occur in a wide variety of environments ranging from experimental and industrial systems on Earth to astrophysical thermonuclear (type Ia) supernovae explosions. Substantial progress has been made in elucidating the nature of DDT in terrestrial confined systems with walls, obstacles, etc., or with pre-existing shocks. It remains unclear, however, whether DDT can occur in unconfined media. Here we show, through first-principles direct numerical simulations (DNS) of the interaction of high-speed turbulence with premixed flames, that at sufficiently high turbulent intensities, subsonic turbulent flames in unconfined environments are inherently susceptible to DDT. The associated mechanism, based on the nonsteady evolution of flames faster than the Chapman-Jouguet deflagrations, is qualitatively different from the traditionally suggested spontaneous reaction wave model, and thus does not require the formation of distributed flames. We show that the critical turbulent flame speed predicted by this mechanism for the onset of DDT is in agreement with DNS results.

15. SUBJECT TERMS

Flames Detonation
Turbulence Combustion

16. SECURITY CLASSIFICATION OF:			**17. LIMITATION OF ABSTRACT**	**18. NUMBER OF PAGES**	**19a. NAME OF RESPONSIBLE PERSON**
					A.Y. Poludnenko
a. REPORT	**b. ABSTRACT**	**c. THIS PAGE**	UL	7	**19b. TELEPHONE NUMBER** *(include area code)*
Unclassified	Unclassified	Unclassified			(202) 767-6582

Standard Form 298 (Rev. 8-98)
Prescribed by ANSI Std. Z39.18

1. Introduction

Since the discovery of the detonation [1, 2], the question of physical mechanisms that create this self-supporting, supersonic, shock-driven reaction wave has been at the forefront of the combustion theory. The development of a detonation is a significant threat to chemical storage and processing facilities, mining operations, etc. [3], while controlled detonation initiation in the next generation of propulsion systems promises to revolutionize transportation [4]. On astrophysical scales, detonation formation is presently believed to be the most important, yet least understood, aspect of the explosion mechanism [5, 6] powering type Ia supernovae (SNIa), the thermonuclear incineration of a degenerate white dwarf star. The use of SNIa as cosmological standard distance indicators has led to the discovery of the accelerating expansion of the Universe [7, 8], suggesting the existence of dark energy. Future high-precision cosmology studies of dark energy will require accurate calibration of SNIa as standard candles, which will be impossible without understanding the process of detonation formation.

Already first systematic studies of detonation showed [2] that it can arise from a slow, highly subsonic deflagration ignited in an initially unpressurized system. Significant progress has since been made experimentally [9, 10] and numerically [11, 12, 13, 14, 15] in elucidating the physics of the deflagration-to-detonation transition (DDT) in confined systems, in particular in closed channels. These studies showed that the confining effect of channel walls on the hot, expanding burning products and the interaction of the resulting flow with walls and obstacles are instrumental in providing significant flame acceleration and pressure increase, thus creating the conditions necessary for detonation ignition. This raises the question: is DDT possible in unconfined media without assistance of walls or obstacles, e.g., in unconfined clouds of fuel vapor or in the interior of a white dwarf during a SNIa explosion?

It was originally suggested by Zel'dovich et al. [16] that a detonation can form in a region (hot spot) with a suitable gradient of reactivity. The resulting spontaneous reaction wave propagating through that gradient creates a pressure wave that can eventually develop into a shock and a detonation [17, 18]. In confined systems, multidimensional direct numerical simulations (DNS) have shown that hot spots can form through repeated shock-flame interactions and fuel compression by shocks [11].

It remains unclear, however, if and how hot spots would form in unconfined, unpressurized media. The most likely mechanism is flame interaction with intense turbulence. In particular, it was suggested [18, 19] that disruption of the internal flame structure by high-speed turbulence, producing a distributed mode of burning, can create hot spots capable of initiating a detonation. It is unknown, however, whether this can indeed occur, as there are no realistic *ab initio* experimental or numerical demonstrations of this process. Here we show that high-speed turbulence-flame interaction can indeed lead to DDT, but through a different process that does not rely on the propagation of a spontaneous reaction wave and, thus, does not require the formation of hot spots.

2. Physical model and numerical method

The DNS calculations presented here solve compressible reactive-flow equations with thermal conduction, molecular species diffusion, and energy release [20, 21]. They use an ideal gas equation of state and first-order Arrhenius kinetics that describes chemical reactions converting fuel into product. A simplified reaction-diffusion model represents stoichiometric H_2-air and CH_4-air mixtures under $Le = 1$ conditions with model parameters calibrated to reproduce both laminar flame and detonation properties [12, 13]. The reaction model for CH_4-air was validated against experimental data on DDT in obstructed channels [13].

Simulations were performed with the code Athena-RFX [20, 21, 22]. It uses a fully unsplit corner transport upwind scheme with PPM spatial reconstruction and the HLLC Riemann solver [23] (see [22] for the detailed tests of the hydrodynamic solver and [20, 21] for the discussion of the reactive-flow extensions). Turbulence driving is implemented via a spectral method [24, 20].

3. Numerical simulations

We consider the interaction of a premixed H_2-air flame with high-speed, steadily driven turbulence. The simulation setup is similar to our previous studies [20, 21], which analyzed the quasi-steady turbulent flame evolution (simulation 6 in Fig. 1). Here we consider a larger system and a higher turbulent intensity (simulation 10 in Fig. 1). The computational domain is a uniform $256 \times 256 \times 4096$ Cartesian mesh with width $L = 0.518$ cm, giving the resolution $\Delta x = \delta_{L,0}/16$, where $\delta_{L,0} \approx 0.032$ cm is the laminar flame thermal width in cold fuel. Kinetic energy is injected at the scale L to produce a homogeneous, isotropic turbulence with characteristic velocity $U = 1.9 \times 10^4$ cm/s $\approx 63 S_{L,0}$ at the scale L, where $S_{L,0} = 3.02 \times 10^2$ cm/s is the laminar flame speed in cold fuel. The corresponding large-scale eddy turnover time is $\tau_{ed} = L/U = 27.3\ \mu$s, while integral velocity $U_l = 1.2 \times 10^4$ cm/s $\approx 40 S_{L,0}$ and integral scale

Manuscript approved May 9, 2011.

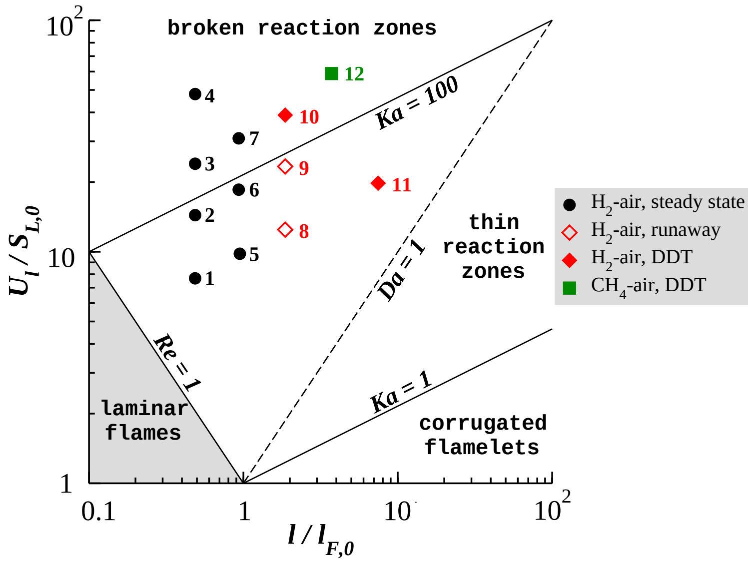

Figure 1: (Color online) Combustion regime diagram [25] showing performed DNS calculations. Symbol color and shape indicate the reactive mixture considered and the observed mode of burning. The full flame width $l_{F,0} \approx 2\delta_{L,0}$ [20].

$l = 0.12$ cm. Resulting turbulence away from the flame has equilibrium Kolmogorov energy spectrum $\propto k^{-5/3}$ in the inertial range extending to scales $\lesssim \delta_{L,0}$ [20].

At $t = 0$, fuel is at the temperature $T_0 = 293$ K and pressure $P_0 = 1.01\times10^6$ erg/cm^3. The planar flame is initialized normal to the longest dimension of the domain (z-axis) with zero-order extrapolation z-boundary conditions and periodic boundaries along other directions. After $\approx 2\tau_{ed}$, the turbulent flame becomes fully developed, and it reaches a quasi-steady state (QSS) which lasts until $t \approx 6.5\tau_{ed}$. Figure 2 shows the turbulent flame speed, S_T, based on the fuel consumption rate [20]. Turbulent flame properties during this period are consistent with the previous analysis of such QSS. In particular, the flame remains in the thin reaction zone regime [20] with the reaction zone structure virtually unaffected by intense turbulence. S_T is primarily controlled by the increase of the flame surface area with the additional occasional increase $\lesssim 30-40\%$ due to periodic flame collisions and the formation of cusps [21].

In contrast with the behavior at a smaller U_l and in a smaller system (case 6), here the QSS lasts a relatively short time (Fig. 2), and after $t \approx 6.5\tau_{ed}$ the flame evolution changes qualitatively: S_T increases rapidly, becoming supersonic by $7.18\tau_{ed}$ and exceeding the Chapman-Jouguet detonation velocity, D_{CJ}, at $7.5\tau_{ed}$. DDT occurs shortly thereafter at $7.53\tau_{ed}$, and S_T reaches its maximum at $7.58\tau_{ed}$. At $7.63\tau_{ed}$ a fully developed overdriven planar detonation emerges, and it quickly relaxes to D_{CJ}.

The system evolution during this process is shown in Fig. 3. At $6.39\tau_{ed}$ a slight overpressure has formed inside the flame brush, and the energy generation rate per unit volume, $\dot{E}$, is still close to its value in the planar laminar flame. As the pressure grows and the turbulent flame accelerates, fuel inside the flame brush is compressed and heated. This increases the local flame speed, S_L, causing $\dot{E}$ to rise. Note, at later times $\dot{E}$ exceeds its laminar value by ~ 2 orders of magnitude. Such accelerated burning leads to further fuel compression and larger S_L. The resulting feedback loop drives a catastrophic runaway process that produces a large pressure build-up and creates strong shocks. Before such shocks are able to form a single global shock, their collision creates a high-pressure triple point that ignites a detonation (details of this last stage will be presented in a separate paper).

To determine the regime of burning during the runaway, we recorded the average temperature, T_f, and pressure, P_f, of pure fuel ($Y \geq 0.95$) inside the flame brush. Up until the moment of DDT, T_f remains < 700 K, and the corresponding induction times are significantly larger than all dynamical timescales. Furthermore, at all times, the average internal flame structure reconstructed using method described in [20] is close to that of a laminar flame in fuel with the corresponding T_f and P_f. Thus, during the runaway, burning is controlled by flame propagation and not by autoignition, which excludes the possibility of formation of global spontaneous reaction waves.

4. Mechanism of the spontaneous runaway

Consider an unconfined fluid volume V with the total internal energy ε. To increase the pressure inside V (as in Fig. 3), an energetic process must generate energy comparable to ε on a characteristic sound-crossing time of this

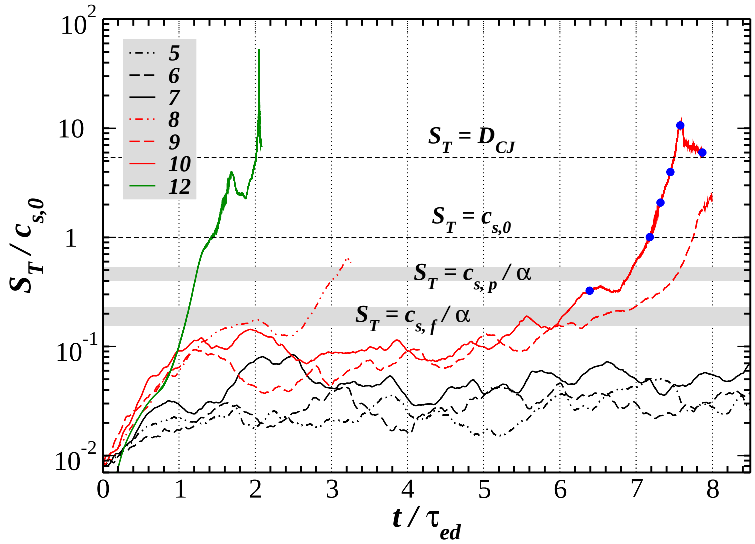

Figure 2: (Color online) Turbulent flame speed, S_T, normalized by the sound speed in cold fuel, $c_{s,0}$. Legend gives simulation numbers (Fig. 1). Shaded gray regions show the range of critical values of S_T according to eq. (1) based on the sound speed in fuel, $c_{s,f}$, and product, $c_{s,p}$, for fuel temperatures in the range 320 − 430 K. Blue dots on the curve for simulation 10 indicate times of individual profiles in Fig. 3. Time is normalized by the corresponding value of τ_{ed} in each simulation.

volume, i.e., $\dot{\varepsilon} \sim \varepsilon/t_s$. If this volume represents a flame with width δ and cross-sectional area L^2, i.e., $V = \delta L^2$, then the burning speed of such flame is defined as $S = \dot{m}/\rho_f L^2$ [20], where $\dot{m} = \dot{\varepsilon}/q$ is the total fuel consumption rate and ρ_f is the fuel density. Then condition $\dot{\varepsilon} \sim \varepsilon/t_s$ can be rewritten as $S \sim c_s E/q\rho_f$, where $t_s = \delta/c_s$, c_s is sound speed, and $E = \varepsilon/V$ is the internal energy per unit volume. The flame here may be laminar, turbulent, or distributed, provided it has the required burning speed.

To show the physical meaning of this condition on S, assume ideal gas equation of state, $E = P/(\gamma - 1)$. At the start of the runaway, pressure is nearly constant across the flame. Then product density is $\rho_p = \rho_f T_f/T_p = \rho_f T_f/(T_f + q/C_p) = P/(P/\rho_f + q(\gamma-1)/\gamma)$, where T_p is the product temperature and C_p is the specific heat at constant pressure. For energetic reactive mixtures, the denominator $P/\rho_f + q(\gamma - 1)/\gamma$ can be approximated as $q(\gamma - 1)$. For instance, in our case, $q = 43.28RT_0/M \gg P_0/\rho_0$, and at the onset of the runaway $P \approx (1.5 - 2)P_0$ and $\rho_f \approx \rho_0$, giving the accuracy of this approximation $\approx 6\% - 11\%$. Thus, $\rho_p \approx P/q(\gamma - 1)$, and we finally get

$$S \sim \frac{c_s}{q\rho_f} E = \frac{c_s}{\rho_f} \frac{P}{q(\gamma - 1)} \approx \frac{c_s}{\alpha} \equiv S_{CJ}, \tag{1}$$

where $\alpha = \rho_f/\rho_p$ is the fluid expansion factor.

In the reference frame of a steady flame, $\rho_p U_p = \rho_f U_f = \rho_f S$, where U_f and U_p are the velocities, respectively, of fuel and product. Thus, eq. (1) is equivalent to the statement that $U_p = c_s$. If c_s is taken to be the sound speed in product then the flame satisfying eq. (1) is a Chapman-Jouguet (CJ) deflagration [26].

The speed of a CJ deflagration, S_{CJ}, is a theoretical maximum for the flame burning speed. The discussion above shows that such a flame generates enough energy on its sound-crossing time to raise its internal pressure and, thus, disrupt its steady-state structure. Real laminar flames, both chemical [26] and thermonuclear [18], do not have burning speeds that approach S_{CJ}. Turbulent flames, however, can develop such high values of S_T.

Unlike a laminar flame, in which local sound speed smoothly increases from its value in fuel, $c_{s,f}$, to that in product, $c_{s,p}$, a turbulent flame effectively consists of two fluids with either $c_{s,f}$ or $c_{s,p}$. Thus, to verify that eq. (1) is indeed the criterion for the onset of runaway, we show in Fig. 2 S_{CJ} based on both $c_{s,f}$ and $c_{s,p}$. Fuel heating by turbulence causes $c_{s,f}$ and $c_{s,p}$ to increase and α to decrease. Shaded gray areas show, for both sound speeds, the range of critical values of S_T corresponding to fuel temperatures 320 − 430 K. In particular, in simulation 10, $T_f \approx 320$ K at $2\tau_{ed}$ (lower bound of the shaded regions) and it increases to ≈ 430 K by $6.5\tau_{ed}$ (upper bound).

Figure 2 shows that upon first reaching the QSS, S_T is close to, but still below, $c_{s,f}/\alpha$, which prevents the onset of the runaway. During the time $(2 - 6.5)\tau_{ed}$, however, fuel heating by turbulence causes S_L to increase by a factor of ≈ 2, thus accelerating S_T above the critical value $c_{s,f}/\alpha$ and allowing the runaway to begin. Figure 3(c) shows that at this point the product velocity indeed becomes $\approx c_{s,f}$. Furthermore, growth rate of S_T increases significantly once S_T

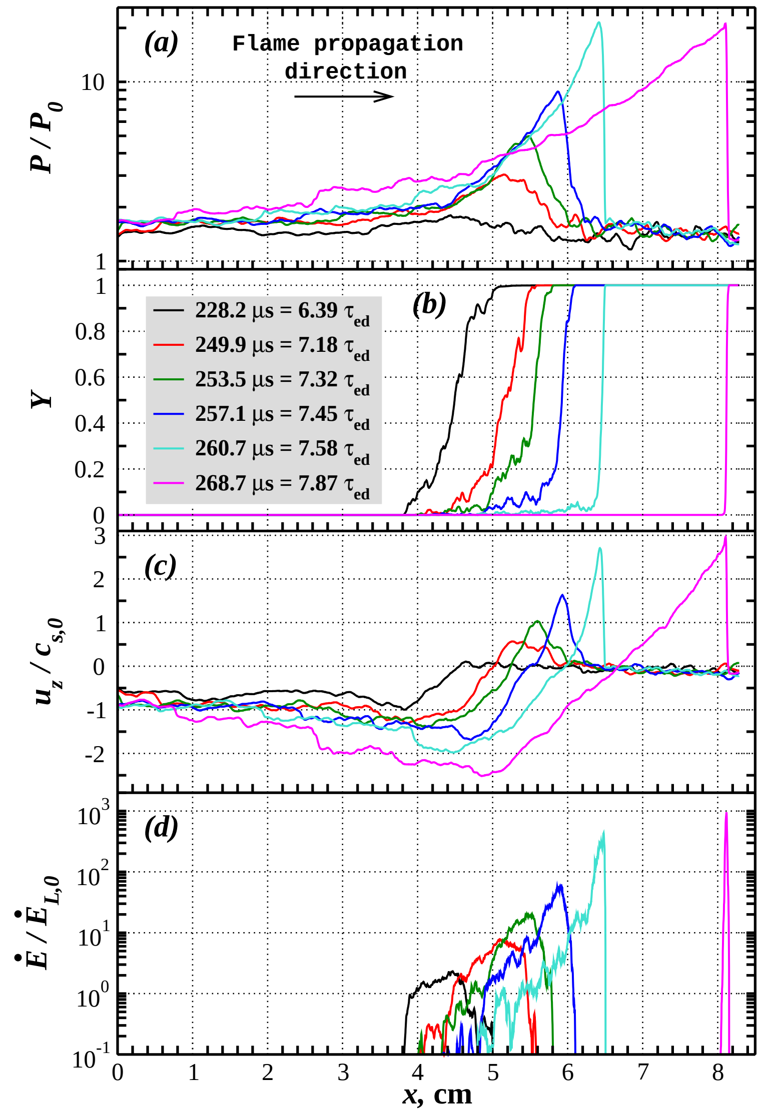

Figure 3: (Color online) The *x*-*y*-averaged profiles of (a) pressure, P, (b) fuel mass fraction, Y, (c) z-velocity, u_z, and (d) energy generation rate per unit volume, $\dot{E}$, in simulation 10. Time since ignition for each profile is shown in panel (b) (these times are indicated with blue dots in Fig. 2). The $\dot{E}$ is normalized by its value in a planar laminar flame propagating in cold fuel, $\dot{E}_{L,0} = qS_{L,0}\rho_0/\delta_{L,0}$, where q is chemical energy release and ρ_0 is cold fuel density.

becomes $> c_{s,p}/\alpha$, i.e., when U_p becomes supersonic relative to both sound speeds. Note also that the transition from a QSS to a detonation occurs, effectively, on a sound-crossing time of the turbulent flame $t_s = \delta_T/c_{s,0} \approx 27\mu\text{s} \approx \tau_{ed}$, where $\delta_T \approx 1$ cm is the flame brush width (Fig. 3b) and $c_{s,0} \approx 3.7 \times 10^4$ cm/s.

For comparison, Fig. 2 also shows S_T for turbulent H_2-air flames for other values of U_l and l (Fig. 1). In particular, in simulations 5-7, S_T remains well below $c_{s,f}/\alpha$ and the flame evolves in the QSS similar to that described in [20, 21]. This QSS was observed over significantly longer periods of time than shown in Fig. 2, e.g., $16\tau_{ed}$ in case 6. Cases 1-4 had similar behavior and, thus, are not shown. We did observe the runaway process in simulations 8 and 9, but in these cases the flame brush accelerated significantly and exited the domain before DDT could occur. The overall growth rate of S_T was lower than in simulation 10 (τ_{ed} increases with decreasing U_l). All simulations are well-resolved with resolution at least $\Delta x = \delta_{L,0}/16$ [20]. Convergence at this resolution was confirmed for the QSS in cases 6 [20, 21] and 7 using resolutions $\Delta x = \delta_{L,0}/8 - \delta_{L,0}/32$, and convergence during the runaway was confirmed in case 10 using resolutions $\Delta x = \delta_{L,0}/8 - \delta_{L,0}/16$. We also observed DDT in simulation 4 which, however, was under-resolved ($\Delta x = \delta_{L,0}/4$) and, thus, is not shown here.

To determine the dependence of our results on the reaction model, we carried out a similar simulation in a stoichiometric CH_4-air mixture. In this case, $\delta_{L,0} = 0.042$ cm is close to that in H_2-air, but the flame speed is almost

an order of magnitude lower, $S_{L,0} = 38$ cm/s [13]. We also observed DDT in this fuel, but only at higher turbulent intensity relative to S_L with $U_l = 2.24 \times 10^3$ cm/s $\approx 59 S_L$ and in a larger system $l = 0.31$ cm ($L = 1.328$ cm) (case 12, Figs. 1 and 2). The overall evolution, however, was different from case 10. The time to DDT was $\approx 2\tau_{ed}$ and the flame never developed a QSS. The flame accelerated significantly relative to fuel, which required a longer domain ($256 \times 256 \times 8192$) to observe DDT, and, in contrast with simulation 10, a strong well-defined global shock was formed. This suggests that there exist two distinct types of flame evolution in such unstable regimes.

The key aspect of the spontaneous DDT mechanism discussed here is that it does not place any specific constraints on the equation of state, reaction model, or the flame properties. Decrease of fluid density with increasing temperature in an exothermic process means that at a sufficiently high but subsonic burning speed, the flow of products will become supersonic, irrespective of how burning occurs. This ensures that the pressure wave remains coupled to the region in which the energy release occurs (cf. location of peaks of P and $\dot{E}$ in Fig. 3b and c). This is in contrast with the spontaneous reaction wave model [16] that requires very specific hot spot properties in order for the resulting reaction wave to remain properly coupled to the pressure pulse that it generates.

Figure 1 suggests that there is both a minimal system size and minimal relative turbulent intensity at which DDT is possible, and their values are not universal as they appear to increase for reactive mixtures with slower laminar flames. Applying the criterion given by eq. (1) to establish whether DDT can occur in a given turbulent flow critically depends on our ability to predict the turbulent flame speed for given U_l and l. This is particularly difficult in the high-speed regimes, and it is in these regimes where spontaneous DDT is most likely to occur.

Acknowledgments

We thank Vadim Gamezo, Craig Wheeler, and Forman Williams for stimulating discussions. This work was supported by the Air Force Office of Scientific Research and by the Office of Naval Research / Naval Research Laboratory.

References

[1] M. Berthelot and P. Vieille, Compt. Rend. Acad. Sci. **93**, 18 (1881).
[2] E. Mallard and H.L. le Chatelier, Compt. Rend. Acad. Sci. **93**, 145 (1881).
[3] M.A. Nettleton, *Gaseous Detonations* (Chapman and Hall, 1987).
[4] G.D. Roy, S.M. Frolov, A.A. Borisov, and D.W. Netzer, Prog. Energy Combust. Sci. **30**, 545 (2004).
[5] A.M. Khokhlov, Astron. Astrophys. **245**, 114 (1991).
[6] V.N. Gamezo, A.M. Khokhlov, and E.S. Oran, Phys. Rev. Lett. **92**, 211102 (2004).
[7] A.G. Riess *et al.*, Astron. J. **116**, 1009 (1998).
[8] S. Perlmutter *et al.*, Astrophys. J. **517**, 565 (1999).
[9] P. Urtiew and A.K. Oppenheim, Proc. Roy. Soc. London Ser. A **295**, 13 (1966).
[10] M. Kuznetsov, M. Liberman, and I. Matsukov, Combust. Sci. Tech. **182**, 1628 (2010).
[11] E.S. Oran and V.N. Gamezo, Combust. Flame **148**, 4 (2007).
[12] V.N. Gamezo, T. Ogawa, and E.S. Oran, Combust. Flame **155**, 302 (2008).
[13] D.A. Kessler, V.N. Gamezo, and E.S. Oran, Combust. Flame **157**, 2063 (2010).
[14] V. Bychkov, D. Valiev, and L.-E. Eriksson, Phys. Rev. Lett. **101**, 164501 (2008).
[15] M.A. Liberman *et al.*, Acta Astronaut. **67**, 688 (2010).
[16] Ya.B. Zel'dovich, V.B. Librovich, G.M. Makhviladze, and G.I. Sivashinsky, Astronaut. Acta **15**, 313 (1970).
[17] A.K. Kapila, D.W. Schwendeman, J.J. Quirk, and T. Hawa, Combust. Theor. Model. **6**, 553 (2002).
[18] A.M. Khokhlov, E.S. Oran, and J.C. Wheeler, Astrophys. J. **478**, 678 (1997).
[19] J.C. Niemeyer and S.E. Woosley, Astrophys. J. **475**, 740 (1997).
[20] A.Y. Poludnenko and E.S. Oran, Combust. and Flame **157**, 995 (2010).
[21] A.Y. Poludnenko and E.S. Oran, Combust. and Flame **158**, 301 (2011).
[22] J.M. Stone *et al.*, Astrophys. J. Supp. **178**, 137 (2008).
[23] T.A. Gardiner and J.M. Stone, J. Comput. Phys. **227**, 4123 (2008).
[24] M.N. Lemaster and J.M. Stone, Astrophys. J. **691**, 1092 (2009).
[25] N. Peters, *Turbulent Combustion* (Cambridge University Press, 2000).
[26] F. Williams, *Combustion Theory* (Perseus Books, 1985).